Signal Transduction in a Covalent Post-Assembly Modification Cascade

Ben S. Pilgrim[1†], Derrick A. Roberts[1†], Thorsten G. Lohr[1], Tanya K. Ronson[1] and Jonathan R. Nitschke[1*]

[1]Department of Chemistry, The University of Cambridge, Lensfield Road, Cambridge CB2 1EW, United Kingdom. [†]These authors contributed equally to this work. [*]e-mail: jrn34@cam.ac.uk.

Natural reaction cascades control the movement of biomolecules between cellular compartments. Inspired by these systems, we report a synthetic reaction cascade employing post-assembly modification reactions to direct the partitioning of supramolecular complexes between phases. The system is comprised of a self-assembled tetrazine-edged $Fe^{II}_8L_{12}$ cube and a maleimide-functionalized $Fe^{II}_4L_6$ tetrahedron. Norbornadiene (NBD) functions as the stimulus that triggers the cascade, beginning with the inverse electron-demand Diels-Alder reaction of NBD with the tetrazine moieties of the cube. This reaction generates cyclopentadiene as a transient by-product, acting as a relay signal that subsequently undergoes a Diels-Alder reaction with the maleimide-functionalized tetrahedron. Cyclooctyne can selectively inhibit the cascade by outcompeting NBD as the initial trigger. Triggering the cascade with 2-octadecylNBD leads to selective alkylation of the tetrahedron upon cascade completion. The increased lipophilicity of the C_{18}-tagged tetrahedron drives this complex into a non-polar phase, allowing its isolation from the initially inseparable mixture of complexes.

Reaction cascades allow information to be relayed[1] from an initial stimulus to an eventual output across relatively long distances within biological systems.[2] Such cascades frequently involve sequences of selective covalent bond forming reactions that act on self-assembled biomolecules, such as the post-translational modification (PTM) of proteins[3] or epigenetic modification of DNA.[4] These cascades, which can be mediated by the action of fleeting signal molecules such as nitric oxide,[5] enable cells to respond dynamically to their environment in response to changing biochemical demands. Inspired by these natural cascades, organic chemists have developed cascade reactions for performing multiple bond-forming processes within a single reaction flask, thereby simplifying synthetic routes to complicated molecules. Recently, some of these cascades have featured supramolecular elements such as container molecules, which act as 'nanoreactors'[6, 7] to facilitate particular steps in the cascade.[8-11] There have also been efforts to include features critical to biological functions, such as inhibition or feedback loops,[12] to develop more complex supramolecular systems that exhibit nuanced responses to transient chemical species. To date, however, none of these supramolecular cascades have harnessed covalent post-assembly modification (PAM) of the supramolecular components as a mechanism for signal transduction.

Covalent PAM reactions must satisfy several prerequisites before they can be successfully employed for the structural alteration of a discrete supramolecular complex: they must be chemoselective, afford near-quantitative yields and proceed under mild conditions to avoid damaging the complex. Due to these stringent requirements, 'click' reactions, such as the strain-promoted Huisgen alkyne–azide cycloaddition[13, 14] or inverse electron-demand Diels-Alder (IEDDA) cycloaddition,[15, 16] have been particularly useful as PAM reactions. To date, covalent PAM of metal-organic complexes[17] has been used to alter the product distribution in systems of self-assembled complexes[18-20] modify solubility properties,[21] stabilize metastable structures,[22] change the nature of a capsule's cavity to control guest binding,[23, 24] generate complex molecular topologies[25-28] and graft molecules of interest onto self-assembled structures.[29] Despite this

versatility, PAM in these previous examples has been exclusively carried out either on individual complexes or *via* orthogonal reactions on different complexes within the same system, rather than *via* the interlinked steps of a cascade. By coupling together multiple PAM reactions into a single sequence, here we demonstrate signal transduction in a supramolecular system to control the movement of a nanometre-sized complex across a phase boundary. This sequence evokes the cellular signalling pathways that drive the translocation of biomolecules across biological membranes.

Results and Discussion

The cascade system developed herein features tetrazine-edged $Fe^{II}_8L_{12}$ cube **1a** and maleimide-functionalized $Fe^{II}_4L_6$ tetrahedron **3**, which undergo a tandem sequence of IEDDA and normal electron-demand Diels-Alder (DA) reactions connected *via* a transient relay signal. The cascade is triggered by the addition of 2-octadecylnorbornadiene (C_{18}-NBD), which undergoes IEDDA reactions on its least-hindered side with the tetrazines of cube **1a** to give pyridazine-edged cube **2** and 1-octadecylcyclopentadiene (C_{18}-CPD) as a metastable intermediate (Fig. 1). The C_{18}-CPD by-product of the first reaction step subsequently acts as a relay signal for the second DA reaction step, in which the maleimide units of tetrahedron **3** are converted into the C_{18}-norbornene moieties of tetrahedron **4d**. In the absence of a C_{18}-NBD trigger, the initial state of the cascade system is stable due to the orthogonal Diels-Alder reactivities of cube **1a** and tetrahedron **3**. The alkyl chains appended to complex **4d** following the cascade render it sufficiently lipophilic to undergo spontaneous phase transfer from a polar organic phase ($CH_3CN/CHCl_3$ 9:1) to a non-polar organic phase (cyclopentane).

Cube **1a** is derived from subcomponent **A**, whose design combines two strategies: the use of a ligand whose twin 4-substituted 2-formylpyridine moieties are arrayed in the correct geometry to generate an M_8L_{12} cubic framework,[30] and the incorporation of 3,6-disubstituted tetrazine spacers into ligand frameworks to enable PAM by IEDDA reactions.[16] Cube **1a** was thus prepared (see Methods) by the subcomponent self-assembly[31] of dialdehyde **A**, which was synthesized in a protecting-group-free three-step sequence (Supplementary Fig. 1),[32-34] *para*-*tert*-butylaniline and iron(II) bis(trifluoromethane)sulfonimide, ($Fe(NTf_2)_2$), in CH_3CN at 333 K for 16 h (Fig. 1). After purification, ESI-MS of the reaction mixture confirmed the formation of an $Fe^{II}_8L_{12}$ complex in solution (Supplementary Fig. 12). ^{1}H NMR analysis of the reaction mixture revealed the formation of a single product having only one signal for each unique ligand environment, consistent with the expected cubic geometry (Supplementary Fig. 10). The high solubility of **1a** in typical non-solvents precluded its crystallization. Fortunately, the lower solubility of cube **1b**, which was prepared using *para*-toluidine in place of 4-*tert*-butylaniline, proved conducive to the growth of single crystals of this complex, obtained by slow vapour diffusion of *i*Pr_2O into a solution of **1b**$[NTf_2]_{16}$ containing $KAsF_6$ (~100 equiv.). X-ray diffraction analysis confirmed complex **1b** to be an achiral $Fe^{II}_8L_{12}$ cube of idealized T_h point group symmetry in the solid state,[30] with adjacent vertices of alternating Λ and Δ handedness (Fig. 2a) (Supplementary Figs 94-96).

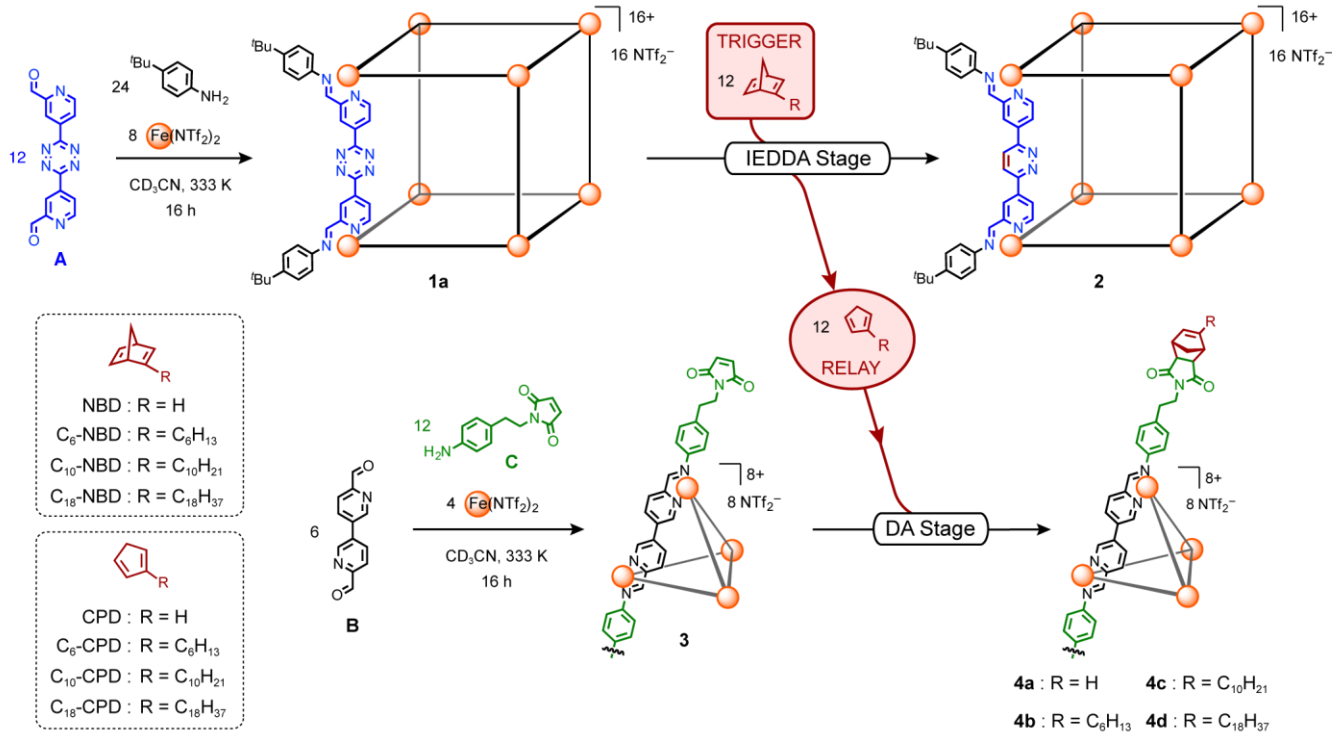

Figure 1 | Overview of syntheses and post-assembly modification cascade. Complexes **1a** and **3** are assembled from dialdehydes **A** and **B** respectively. The PAM cascade proceeds *via* inverse electron-demand Diels-Alder and subsequent normal electron-demand Diels-Alder reactions to convert **1a** and **3** into complexes **2** and **4(a-d)** respectively.

Tetrahedron **3**, functionalized with pendant maleimide groups, was designed as a suitable reaction partner for the alkylated-CPD relay signal released from the IEDDA reaction in the first step, which required the synthesis of novel maleimide-functionalized aniline **C**. This aniline features an ethylene spacer to reduce steric congestion at the vertices of the tetrahedron. Aniline **C** was prepared in three steps from commercially-available starting materials (Supplementary Fig. 26).[35] Tetrahedron **3** was subsequently prepared (see Methods) by subcomponent self-assembly of dialdehyde **B**,[36] aniline **C**, and iron(II) bis(trifluoromethane)sulfonimide, ($Fe(NTf_2)_2$) in CH_3CN at 333 K for 16 h (Fig. 1). Slow vapour diffusion of *i*Pr_2O into a CH_3CN solution of **3** containing Bu_4NPF_6 (~100 equiv.) yielded single crystals suitable for X-ray diffraction analysis, unambiguously confirming the *T*-symmetric framework of **3** in the solid state (Fig. 2b), echoing the results of solution ESI-MS and ^{1}H NMR analyses (Supplementary Figs 35 and 38).

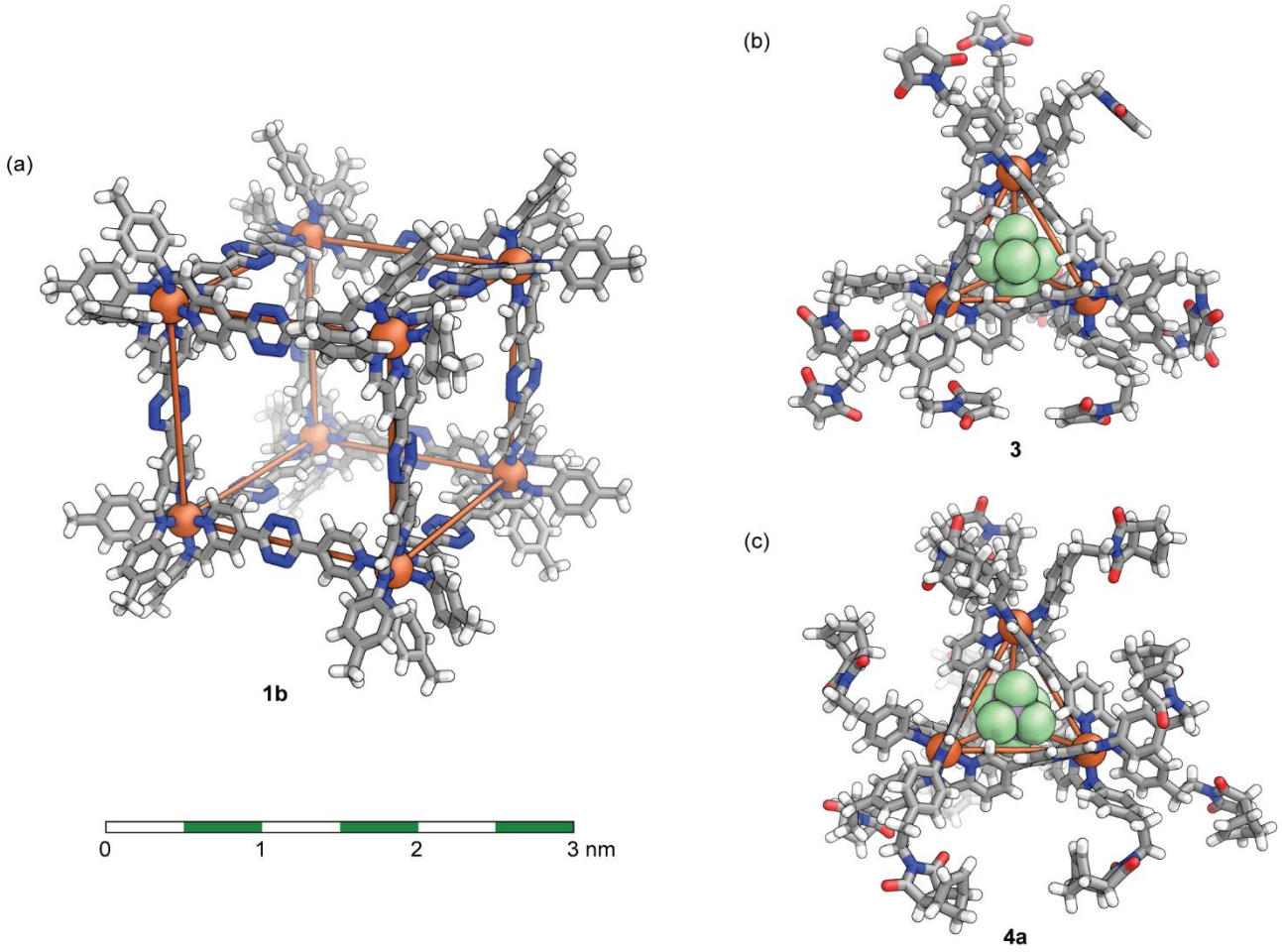

Figure 2 | Depictions (same scale) of the X-ray crystal structures. a. Cube **1b**. **b.** The PF_6^- adduct of tetrahedron **3**. **c.** The AsF_6^- adduct of modified tetrahedron **4a**. Key: grey = carbon, white = hydrogen, red = oxygen, blue = nitrogen, orange = iron, light green = fluorine. Disorder and non-encapsulated anions have been omitted for clarity. Iron atoms are connected with orange lines to illustrate the overall geometry of each complex.

Before investigating the PAM cascade with an alkylated-NBD, we first tested its viability in a model system using commercially-available, unsubstituted NBD. In this model system, the relay signal CPD could also be easily prepared by cracking dicyclopentadiene, allowing the IEDDA and DA steps to be examined in isolation to afford pure samples of both product complexes **2** and **4a** for characterization purposes.

The reaction of cube **1a** with NBD (16 equiv. per cube) proceeded cleanly to furnish dodecafunctionalized pyridazine-edged cube **2** as the only supramolecular product, alongside the CPD by-product, within 4 h, as verified by ^{1}H NMR and ESI-MS analyses (Supplementary Figs 41 and 42). At intermediate time points, desymmetrization of the cage signals was observed; however, the characteristic signals from the vertex protons on the complex persisted and no signals from free subcomponents appeared, suggesting that the ligands did not dissociate from the cage during this reaction sequence.[16] To test the reactivity of tetrahedron **3** towards the CPD relay signal in isolation, freshly distilled CPD (16 equiv. per tetrahedron) was added to a CD_3CN solution of **3**, leading to the clean formation of norbornene-grafted **4a**, as confirmed by both ESI-MS and ^{1}H NMR analyses (Supplementary Figs 44 and 47). Slow vapour diffusion of *i*Pr_2O into a CD_3CN solution of **4a** containing $KAsF_6$ (~100 equiv.) yielded single crystals suitable for X-ray diffraction, the analysis of which confirmed the *T*-symmetric framework of **4a** in the solid state and that DA reactions had

taken place with *endo* selectivity (Fig. 2c). Both complexes **3** and **4a** contained a single encapsulated anion (PF_6^- or AsF_6^-) in the crystal structure, consistent with the behaviours of other tetrahedra constructed from dialdehyde **B**.[36] In batches of tetrahedron **3** synthesized with 1.0 equiv. of NMe_4PF_6, the encapsulation of PF_6^- in the solution phase was verified by ^{19}F NMR (Supplementary Fig. 37). Samples of **4a** derived from the PAM of such batches of **3** also exhibited PF_6^- encapsulation in solution (Supplementary Fig. 46), confirming that PAM does not disrupt the guest binding behaviour of the tetrahedral framework.

The full IEDDA-DA PAM cascade in this model system was initiated by the addition of NBD (30 equiv. per **1a**) to a mixture of cube **1a** and tetrahedron **3** in CD_3CN at 293 K. *In situ* ^1H NMR analysis of the reaction (Fig. 3a) showed that the IEDDA pathway proceeded rapidly upon addition of NBD to the system, resulting in a decrease in the signals corresponding to **1a** and concomitant appearance of cube **2** and CPD. As the concentration of CPD grew, the secondary DA reaction proceeded, resulting in clean conversion of **3** to **4a**. The sharpness of the signals from **2** and **4a** at the end of the reaction indicated the absence of ligand scrambling, further supporting our inference that the complexes remain intact during the PAM cascade.

We note that CPD is a metastable intermediate and will dimerise in the absence of an alternative reactive partner. It is produced here only in a small quantity, akin to the transient nitric oxide signals employed by biological systems.[5] It would not be straightforward to extract the CPD from a system containing only it and cube **2**, and then use it to modify either aniline **C** pre-self-assembly or tetrahedron **3** post-self-assembly. This observation highlights a particularly useful feature of a cascade approach to PAM, since the *in situ* formation of CPD overcomes the challenges of synthesising and isolating alkyl-substituted CPDs (*vide infra*). As expected, when NBD was added to tetrahedron **3** in isolation, or CPD added to cube **1a** in isolation, no reaction was observed due to the sequence dependence of the cascade.

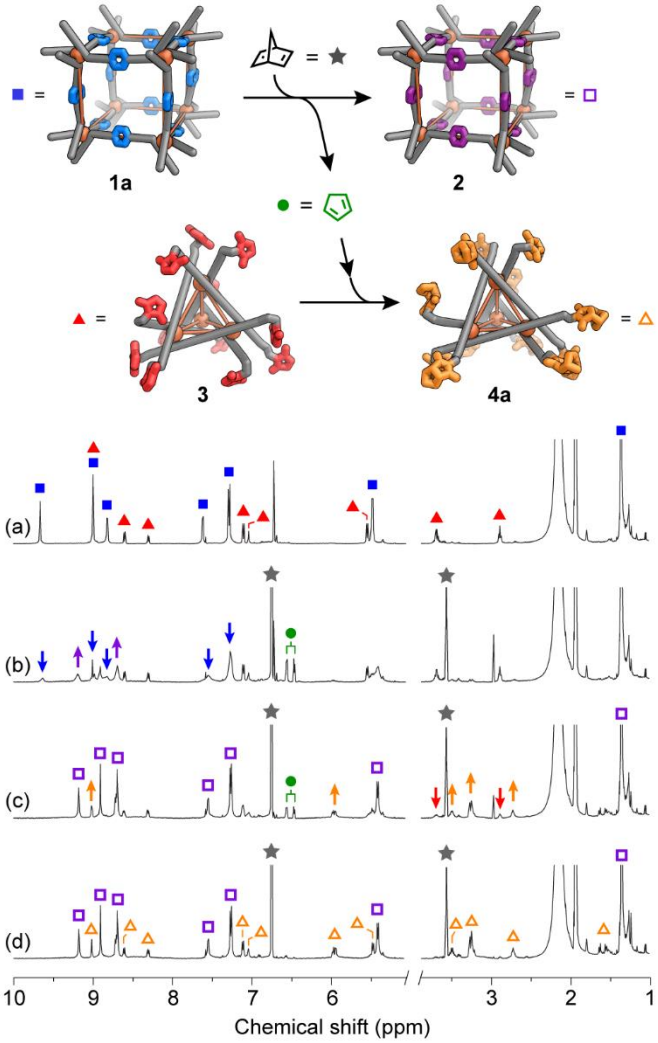

Figure 3 | Monitoring the model post-assembly modification cascade. ^{1}H NMR (500 MHz, 298 K, CD_3CN) spectra from *in situ* monitoring of the model cascade with CPD (carried out at 293 K) at various time points are shown. Signals are marked as follows: tetrazine cube **1a** (solid blue squares), pyridazine cube **2** (hollow purple squares), maleimide tetrahedron **3** (solid red triangles), norbornene tetrahedron **4a** (hollow orange triangles), NBD (grey stars), CPD (green circles). **a.** Spectrum before addition of NBD. **b.** Spectrum 30 min after NBD addition, with IEDDA step well underway. **c.** Spectrum 4 h after NBD addition, with IEEDA step largely complete and DA step well underway. **d.** Spectrum 22 h after NBD addition, with both steps complete.

A hallmark of biological systems is their ability to respond to different signals in specific ways, with certain signals overriding others to inhibit a process. Cyclooctyne was shown to function as an inhibitor within the context of our PAM cascade system: when a solution of NBD (18 equiv. per cube) and cyclooctyne (12 equiv. per cube) was added to an equimolar mixture of cube **1a** and tetrahedron **3** in CD_3CN, the more reactive cyclooctyne underwent IEDDA preferentially with complex **1a**, affording cyclooctylpyridazine-edged complex **5** as the only observed product within minutes of addition (Fig. 4) (Supplementary Figs 58-62). Because NBD was prevented from reacting with **1a**, no relay CPD signal was produced, thus inhibiting the cascade and showing how a more reactive signal can override a less reactive one.

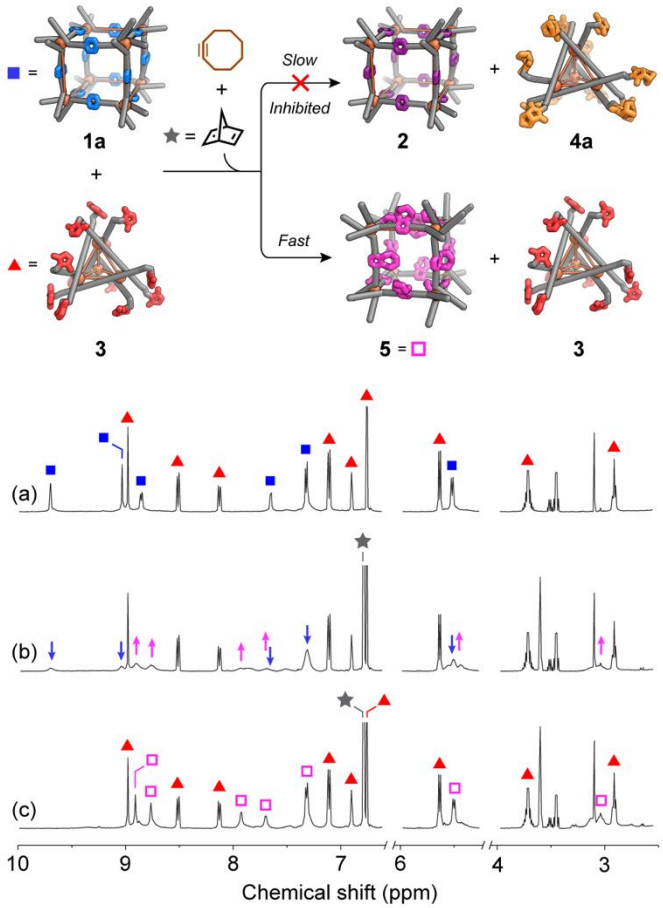

Figure 4 | Monitoring the inhibited post-assembly modification cascade. ^{1}H NMR (500 MHz, 298 K, CD_3CN) spectra from *in situ* monitoring of the inhibited cascade (carried out at 293 K) at various time points are shown. Signals are marked as follows: tetrazine cube **1a** (solid blue squares), pyridazine cube **5** (hollow pink squares), maleimide tetrahedron **3** (red triangles), NBD (grey stars). **a.** Spectrum before addition of NBD/cyclooctyne. **b.** Spectrum 3 min after NBD/cyclooctyne addition **c.** Spectrum 8 min after NBD/cyclooctyne addition.

To translate the effects of the microscopic PAM cascade to the macroscopic regime, we sought to couple PAM to a phase transition whereby tetrahedron **4** would be rendered sufficiently lipophilic to spontaneously move into a non-polar solvent upon completion of the cascade. Three NBDs of increasing alkyl chain length —2-hexyl-NBD (C_6-NBD), 2-decyl-NBD (C_{10}-NBD) and 2-octadecyl-NBD (C_{18}-NBD)—were synthesized (Supplementary Fig. 64) as triggers for the cascade. The cascade reactions were performed in either CH_3CN (for C_6-NBD) or a 9:1 mixture of CH_3CN:$CHCl_3$ (for C_6-NBD, C_{10}-NBD and C_{18}-NBD) as the polar 'reaction' phase, with the $CHCl_3$ added to help solubilize the more lipophilic alkyl-NBDs. Cyclopentane was selected as the non-polar 'destination' phase for extracting the alkylated tetrahedra, because it is immiscible with the aforementioned polar phases and neither cage **1a** nor **3** was observed to partition into cyclopentane from either CH_3CN or 9:1 $CH_3CN/CHCl_3$. The cascade was initiated by the addition of the appropriate NBD to a mixture of **1a** and **3** (see Methods). After the reaction was judged complete by ^{1}H NMR analysis, an equal volume of cyclopentane was added, the mixture shaken in a vortex mixer to enable phase transfer; the phases were then separated by centrifugation.

Addition of C_6-NBD to the system of **1** and **3a** in CD_3CN (or in a 9:1 $CD_3CN/CDCl_3$ mixture) resulted in clean conversions after 20-24 h at 293 K to cube **2** and tetrahedron **4b** respectively. The cyclopentane phase remained colourless following attempted extraction, however, indicating that tetrahedron **4b** failed to

partition into cyclopentane. With C_{10}-NBD in 9:1 $CD_3CN/CDCl_3$, clean conversions to cube **2** and tetrahedron **4c** were also observed by ^{1}H NMR, but tetrahedron **4c** also failed to partition into cyclopentane following attempted extraction. However, with C_{18}-NBD in 9:1 $CD_3CN/CDCl_3$, clean conversions of **1** and **3a** to cube **2** and tetrahedron **4d** were followed by successful extraction into cyclopentane, as evidenced by the deep purple colour of the cyclopentane layer (Fig. 5c).

This coloured cyclopentane layer was decanted and a further extraction performed with fresh cyclopentane. The second cyclopentane extract was much paler in colour, indicating almost all tetrahedron **4d** underwent phase transfer upon the first extraction. The cyclopentane was not noticeably coloured following attempted extraction for the third time. Analysis of the remaining $CD_3CN/CDCl_3$ layer from the cascade by ^{1}H NMR showed exclusively the presence of cube **2** (Supplementary Fig. 87). The first two cyclopentane extracts were combined, concentrated and the residue dissolved in 1:1 $CD_3CN/CDCl_3$, whereby ^{1}H NMR analysis revealed the presence of tetrahedron **4d** only, confirming that this complex retained its structural integrity following successful transfer into a non-polar solvent phase. In cases where tetrahedron **3** contained encapsulated PF_6^- prior to initiation of the reaction cascade, ^{19}F NMR analysis of tetrahedron **4d** isolated after this phase transition indicated PF_6^- was still encapsulated (Supplementary Fig. 91). This experiment thus demonstrates the possibility of signal transduction in a synthetic system over large distances, whereby tetrahedron **4d** crosses a macroscopic phase boundary with the cargo present in tetrahedron **3** before PAM also present in tetrahedron **4d** after PAM and subsequent phase switching.

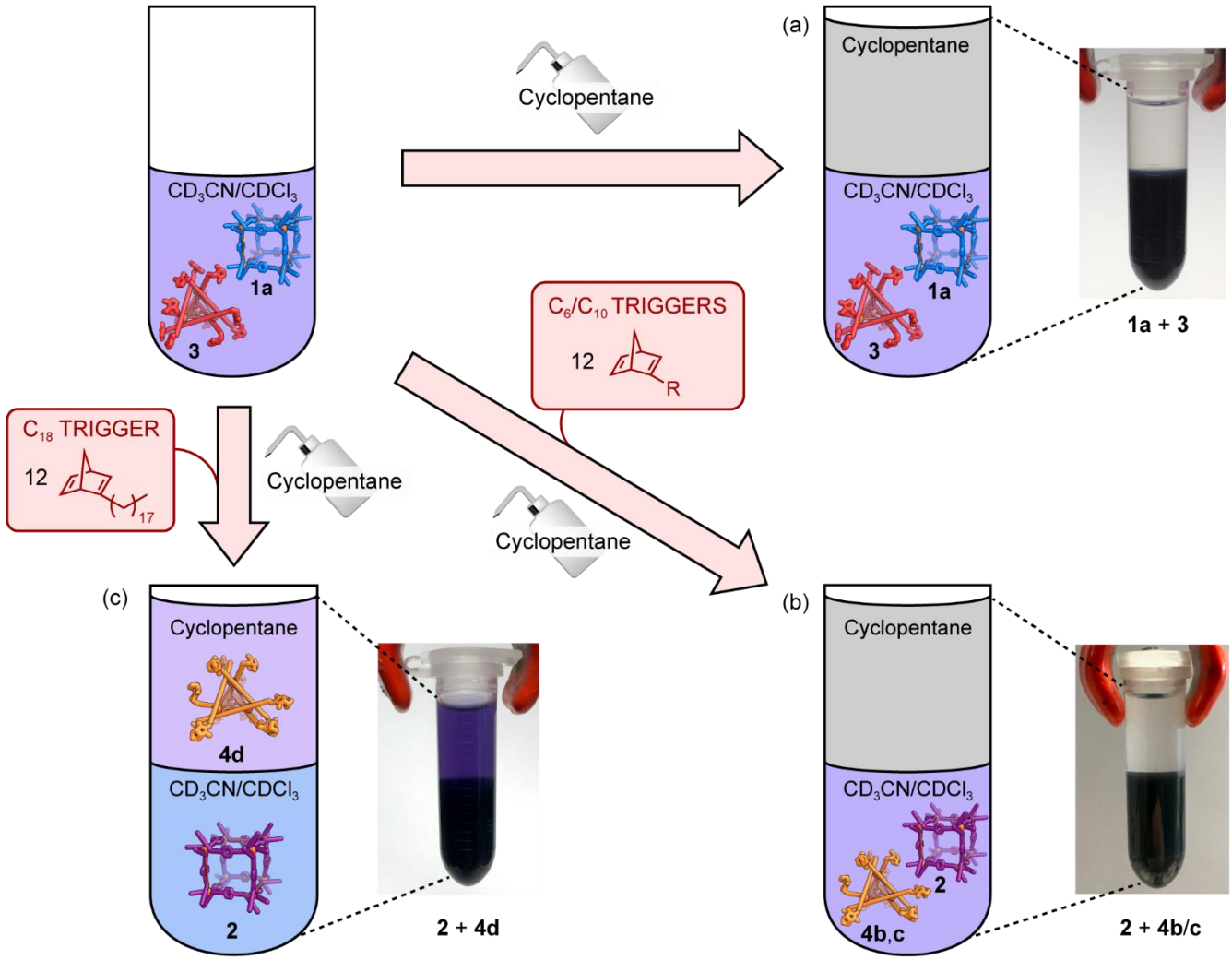

Figure 5 | Signal transduction leading to phase segregation of the two product complexes. **a.** No transitioning of the starting complexes **1a** and **3** to the non-polar phase occurred, rendering them inseparable before application of the NBD signal. **b.** The C_6-NBD or C_{10}-NBD signals did not render the tetrahedra **4b** or **4c** sufficiently lipophilic to induce transfer into a non-polar phase. **c.** The C_{18}-NBD signal-induced transfer of tetrahedron **4d** into a non-polar phase upon completion of the PAM cascade.

Summary and Outlook

Natural PTM cascade reactions underpin the ability of cells to dynamically regulate their activities in response to external stimuli. We propose that covalent PAM could serve an analogous role in supramolecular chemistry, enabling the construction of stimuli-responsive chemical systems[37-39] that emulate the functional diversity of their biological counterparts. The two-step PAM cascade presented herein, for which the functional response is the transition of a large supramolecular structure across a phase boundary, demonstrates this proposition. This cascade system, which responds to a triggering signal (NBD), employs a relay shuttle (CPD) and can be interrupted by an inhibitor (cyclooctyne), functionally mirrors many of the key features of the complex signal transduction pathways of biology, but in an entirely abiological context. Such systems have clear potential to transport cargo across phase boundaries[40] in response to chemical signals. Such a capability may be of use in designing new chemical separations[41] inspired by the scale[42-45] and the structural[46-48] and functional complexity[49, 50] of natural signal transduction pathways.

Methods

Self-assembly of cube 1a

A suspension of tetrazine dialdehyde **A** (13.8 mg, 47.1 μmol) and 4-*tert*-butylaniline (14.1 mg, 94.2 μmol) in dry CH_3CN (2.4 mL) was deoxygenated by bubbling nitrogen gas through it for 15 min. Iron(II) bis(trifluoromethylsulfonyl)imide (22.1 mg, 31.4 μmol) was added, after which the solution turned dark blue-green. The resulting mixture was heated to 333 K for 16 h, then cooled to room temperature, filtered through a glass fibre filter (0.7 μm pore size) and then evaporated to dryness under a stream of nitrogen gas. The solid was redissolved in CH_2Cl_2/CH_3CN (95:5) and purified by size exclusion chromatography (Biobeads SX-1), eluting with CH_2Cl_2/CH_3CN (95:5). The main blue-green band was collected, the solvent removed under a stream of nitrogen gas to furnish cube **1a** (41.9 mg, 3.61 μmol, 92%) as a fine dark-blue powder.

Self-assembly of tetrahedron 3

A suspension of dialdehyde **B** (10.8 mg, 50.9 μmol) and aniline **C** (22.0 mg, 102 μmol) in dry CH_3CN (2.5 mL) was deoxygenated by bubbling nitrogen gas through it for 15 min. Iron(II) bis(trifluoromethylsulfonyl)imide (24.0 mg, 33.9 μmol) was added, after which the solution turned purple. The resulting mixture was heated at 333 K for 16 h, then cooled to room temperature, filtered through a glass fibre filter (0.7 μm pore size) and then evaporated to dryness under a stream of nitrogen gas. *i*Pr_2O (20 mL) was then added, the residue re-suspended and then centrifuged (5 min, 3000 rpm) and the *i*Pr_2O decanted. This procedure was repeated with fresh *i*Pr_2O. The residue was then dried *in vacuo* to furnish tetrahedron **3** (42.7 mg, 6.98 μmol, 82%) as a fine purple powder.

Post-assembly modification cascade and subsequent phase separation

A 2 mL microcentrifuge tube was charged with a solution of cube **1a** (2.0 mg, 0.17 μmol, 1.1 equiv.) and tetrahedron **3** (1.0 mg, 0.16 μmol, 1.0 equiv.) in CD_3CN (0.9 mL). A solution of C_{18}-NBD (2.7 mg, 7.9 μmol, 50 equiv.) in $CDCl_3$ (0.1 mL) was added, the reaction mixture homogenized by vortex mixing for 30 s, and the solution was transferred to an NMR tube for *in situ* ^{1}H NMR monitoring. The reaction was performed at 293 K and reached completion after 22 h. The reaction mixture was transferred to a 2 mL microcentrifuge tube, cyclopentane (1 mL) was added, the mixture homogenized by vortex mixing for 30 s, and then the layers separated by centrifugation (9000 rpm, 30-60 sec). Partitioning of the alkylated tetrahedron **4d** into the less dense cyclopentane layer was assessed by visual inspection, as evidenced by the characteristic purple colour of the cyclopentane layer (Supplementary Fig. 89). Tetrahedron **4d** was extracted completely from the $CD_3CN/CDCl_3$ cascade medium by an additional 1 mL extraction into cyclopentane. Complete separation of cube **2** and tetrahedron **4d** into polar and non-polar organic phases respectively, was verified by ^{1}H NMR analysis of the isolated phases. ^{1}H NMR samples were prepared by evaporating each isolated phase to dryness with a stream of nitrogen gas and then redissolving the residue in an appropriate solvent. The remnants of the more polar $CD_3CN/CDCl_3$ phase were redissolved in CD_3CN which revealed the exclusive presence of cube **2**. The remnants of what had transferred to the cyclopentane phase were redissolved in 1:1 $CD_3CN/CDCl_3$, which revealed the exclusive presence of tetrahedron **4d** (Supplementary Fig. 87).

Data Availability

Crystallographic data for the structures reported in this paper have been deposited at the Cambridge Crystallographic Data Centre, under the deposition numbers 1520129-1520131. Copies of these data can be obtained free of charge via www.ccdc.cam.ac.uk/data_request/cif. All other data supporting the findings

of this study are available within the Article and its Supplementary Information, or from the corresponding author upon reasonable request**.**

References

1. Kholodenko, B.N. Cell-signalling dynamics in time and space. *Nat. Rev. Mol. Cell Biol.* **7**, 165-176 (2006).
2. Snider, N.T. & Omary, M.B. Post-translational modifications of intermediate filament proteins: mechanisms and functions. *Nat. Rev. Mol. Cell Biol.* **15**, 163-177 (2014).
3. Deribe, Y.L., Pawson, T. & Dikic, I. Post-translational modifications in signal integration. *Nat. Struct. Mol. Biol.* **17**, 666-672 (2010).
4. Goldberg, A.D., Allis, C.D. & Bernstein, E. Epigenetics: A Landscape Takes Shape. *Cell* **128**, 635-638 (2007).
5. Thomas, D.D. *et al.* The chemical biology of nitric oxide: Implications in cellular signaling. *Free. Radic. Biol. Med.* **45**, 18-31 (2008).
6. Wang, Q.-Q. *et al.* Self-assembled nanospheres with multiple endohedral binding sites pre-organize catalysts and substrates for highly efficient reactions. *Nat. Chem.* **8**, 225-230 (2016).
7. Cullen, W., Misuraca, M.C., Hunter, C.A., Williams, N.H. & Ward, M.D. Highly efficient catalysis of the Kemp elimination in the cavity of a cubic coordination cage. *Nat. Chem.* **8**, 231-236 (2016).
8. Kaphan, D.M., Levin, M.D., Bergman, R.G., Raymond, K.N. & Toste, F.D. A supramolecular microenvironment strategy for transition metal catalysis. *Science* **350**, 1235-1238 (2015).
9. Zhang, Q. & Tiefenbacher, K. Terpene cyclization catalysed inside a self-assembled cavity. *Nat. Chem.* **7**, 197-202 (2015).
10. Wang, Z.J., Clary, K.N., Bergman, R.G., Raymond, K.N. & Toste, F.D. A supramolecular approach to combining enzymatic and transition metal catalysis. *Nat. Chem.* **5**, 100-103 (2013).
11. Salles, A.G., Zarra, S., Turner, R.M. & Nitschke, J.R. A Self-Organizing Chemical Assembly Line. *J. Am. Chem. Soc.* **135**, 19143-19146 (2013).
12. Pramanik, S. & Aprahamian, I. Hydrazone Switch-Based Negative Feedback Loop. *J. Am. Chem. Soc.* **138**, 15142-15145 (2016).
13. Lutz, J.-F. 1,3-Dipolar Cycloadditions of Azides and Alkynes: A Universal Ligation Tool in Polymer and Materials Science. *Angew. Chem. Int. Ed.* **46**, 1018-1025 (2007).
14. Agard, N.J., Baskin, J.M., Prescher, J.A., Lo, A. & Bertozzi, C.R. A Comparative Study of Bioorthogonal Reactions with Azides. *ACS Chem. Biol.* **1**, 644-648 (2006).
15. Foster, R.A.A. & Willis, M.C. Tandem inverse-electron-demand hetero-/retro-Diels-Alder reactions for aromatic nitrogen heterocycle synthesis. *Chem. Soc. Rev.* **42**, 63-76 (2013).
16. Roberts, D.A. *et al.* Post-assembly Modification of Tetrazine-Edged FeII4L6 Tetrahedra. *J. Am. Chem. Soc.* **137**, 10068-10071 (2015).
17. Wang, W., Wang, Y.-X. & Yang, H.-B. Supramolecular transformations within discrete coordination-driven supramolecular architectures. *Chem. Soc. Rev.* **45**, 2656-2693 (2016).
18. Young, M.C., Johnson, A.M. & Hooley, R.J. Self-promoted post-synthetic modification of metal-ligand M2L3 mesocates. *Chem. Commun.* **50**, 1378-1380 (2014).
19. Roberts, D.A., Castilla, A.M., Ronson, T.K. & Nitschke, J.R. Post-assembly Modification of Kinetically Metastable FeII2L3 Triple Helicates. *J. Am. Chem. Soc.* **136**, 8201-8204 (2014).
20. Glasson, C.R.K. *et al.* Post-Assembly Covalent Di- and Tetracapping of a Dinuclear [Fe2L3]4+ Triple Helicate and Two [Fe4L6]8+ Tetrahedra Using Sequential Reductive Aminations. *Inorg. Chem.* **54**, 6986-6992 (2015).
21. Zhao, D. *et al.* Surface Functionalization of Porous Coordination Nanocages Via Click Chemistry and Their Application in Drug Delivery. *Adv. Mater.* **23**, 90-93 (2011).
22. Kaucher, M.S., Harrell, W.A. & Davis, J.T. A Unimolecular G-Quadruplex that Functions as a Synthetic Transmembrane Na+ Transporter. *J. Am. Chem. Soc.* **128**, 38-39 (2006).
23. Schneider, M.W., Oppel, I.M., Griffin, A. & Mastalerz, M. Post-Modification of the Interior of Porous Shape-Persistent Organic Cage Compounds. *Angew. Chem. Int. Ed.* **52**, 3611-3615 (2013).

24. Ronson, T.K., Pilgrim, B.S. & Nitschke, J.R. Pathway-Dependent Post-assembly Modification of an Anthracene-Edged MII4L6 Tetrahedron. *J. Am. Chem. Soc.* **138**, 10417-10420 (2016).
25. Marcos, V. *et al.* Allosteric initiation and regulation of catalysis with a molecular knot. *Science* **352**, 1555-1559 (2016).
26. Meyer, C.D., Joiner, C.S. & Stoddart, J.F. Template-directed synthesis employing reversible imine bond formation. *Chem. Soc. Rev.* **36**, 1705-1723 (2007).
27. Crowley, J.D., Goldup, S.M., Lee, A.-L., Leigh, D.A. & McBurney, R.T. Active metal template synthesis of rotaxanes, catenanes and molecular shuttles. *Chem. Soc. Rev.* **38**, 1530-1541 (2009).
28. Wood, C.S., Ronson, T.K., Belenguer, A.M., Holstein, J.J. & Nitschke, J.R. Two-stage directed self-assembly of a cyclic [3]catenane. *Nat. Chem.* **7**, 354-358 (2015).
29. Chakrabarty, R. & Stang, P.J. Post-assembly Functionalization of Organoplatinum(II) Metallacycles via Copper-free Click Chemistry. *J. Am. Chem. Soc.* **134**, 14738-14741 (2012).
30. Browne, C., Brenet, S., Clegg, J.K. & Nitschke, J.R. Solvent-Dependent Host–Guest Chemistry of an Fe8L12 Cubic Capsule. *Angew. Chem. Int. Ed.* **52**, 1944-1948 (2013).
31. Chakrabarty, R., Mukherjee, P.S. & Stang, P.J. Supramolecular Coordination: Self-Assembly of Finite Two- and Three-Dimensional Ensembles. *Chem. Rev.* **111**, 6810-6918 (2011).
32. Duncton, M.A.J. Minisci reactions: Versatile CH-functionalizations for medicinal chemists. *Med. Chem. Commun.* **2**, 1135-1161 (2011).
33. Audebert, P. *et al.* Synthesis of new substituted tetrazines: electrochemical and spectroscopic properties. *New J. Chem.* **28**, 387-392 (2004).
34. Li, Z. & Ding, J. Bisfuran-s-Tetrazine-Based Conjugated Polymers: Synthesis, Characterization, and Photovoltaic Properties. *Macromol. Chem. Phys.* **212**, 2260-2267 (2011).
35. Hagiya, K., Muramoto, N., Misaki, T. & Sugimura, T. DMEAD: a new dialkyl azodicarboxylate for the Mitsunobu reaction. *Tetrahedron* **65**, 6109-6114 (2009).
36. Hristova, Y.R., Smulders, M.M.J., Clegg, J.K., Breiner, B. & Nitschke, J.R. Selective anion binding by a "Chameleon" capsule with a dynamically reconfigurable exterior. *Chem. Sci.* **2**, 638-641 (2011).
37. Li, L. *et al.* Multiple stimuli-responsive supramolecular gels constructed from metal-organic cycles. *Polym. Chem.* **7**, 6288-6292 (2016).
38. Han, M. *et al.* Light-Controlled Interconversion between a Self-Assembled Triangle and a Rhombicuboctahedral Sphere. *Angew. Chem. Int. Ed.* **55**, 445-449 (2016).
39. Tashiro, S. & Shionoya, M. Stimuli-responsive Synthetic Metallopeptides. *Chem. Lett.* **42**, 456-462 (2013).
40. Ko, S.-K. *et al.* Synthetic ion transporters can induce apoptosis by facilitating chloride anion transport into cells. *Nat. Chem.* **6**, 885-892 (2014).
41. Sholl, D.S. & Lively, R.P. Seven chemical separations to change the world. *Nature* **532**, 435-437 (2016).
42. Fujita, D. *et al.* Self-assembly of tetravalent Goldberg polyhedra from 144 small components. *Nature* **540**, 563-566 (2016).
43. Jansze, S.M., Wise, M.D., Vologzhanina, A.V., Scopelliti, R. & Severin, K. PdII2L4-type coordination cages up to three nanometers in size. *Chem. Sci.*, 10.1039/C1036SC04732G (2017).
44. Fujita, D. *et al.* Self-Assembly of M30L60 Icosidodecahedron. *Chem* **1**, 91-101 (2016).
45. Pilgrim, Ben S. & Nitschke, Jonathan R. That's No Moon: It's a Molecular Capsule. *Chem* **1**, 19-21 (2016).
46. Kim, T. *et al.* Selective Synthesis of Molecular Borromean Rings: Engineering of Supramolecular Topology via Coordination-Driven Self-Assembly. *J. Am. Chem. Soc.* **138**, 8368-8371 (2016).
47. Tanaka, K., Tengeiji, A., Kato, T., Toyama, N. & Shionoya, M. A Discrete Self-Assembled Metal Array in Artificial DNA. *Science* **299**, 1212-1213 (2003).
48. Rizzuto, F.J. & Nitschke, J.R. Stereochemical plasticity modulates cooperative binding in a CoII12L6 cuboctahedron. *Nat. Chem.* **advance online publication** (2017).

49. Ward, M.D. & Raithby, P.R. Functional behaviour from controlled self-assembly: challenges and prospects. *Chem. Soc. Rev.* **42**, 1619-1636 (2013).
50. Zheng, W. *et al.* Construction of Smart Supramolecular Polymeric Hydrogels Cross-linked by Discrete Organoplatinum(II) Metallacycles via Post-Assembly Polymerization. *J. Am. Chem. Soc.* **138**, 4927-4937 (2016).

Acknowledgements

B.S.P. acknowledges the Herchel Smith Research Fellowship, the Royal Commission for the Exhibition of 1851 Research Fellowship and the Fellowship from Corpus Christi College, Cambridge. D.A.R. acknowledges support from the Gates Cambridge Trust. This work was also supported by the UK Engineering and Physical Sciences Research Council (EPSRC, EP/M008258/1). The authors thank Diamond Light Source (UK) for synchrotron beamtime on I19 (MT11397), the NMR facility at the University of Cambridge Chemistry Department, and the EPSRC UK National Mass Spectrometry Facility at Swansea University.

Author Contributions

B.S.P., D.A.R. and J.R.N. conceived the initial ideas for the project. B.S.P. and D.A.R. designed the complexes. B.S.P., D.A.R. and T.G.L. performed the synthetic work. B.S.P. and D.A.R. characterized the compounds, performed the cascades and grew the single crystals. T.K.R. collected diffraction data, and solved and refined the X-ray crystal structures. B.S.P. prepared the initial draft of the paper and all authors contributed to the final draft of the paper.

Additional information

Supplementary information is available in the online version of the paper. Reprints and permissions information is available online at www.nature.com/reprints. Correspondence and requests for materials should be addressed to J.R.N.

Competing financial interests

The authors declare no competing financial interests.